Special Issue: Research Article

polymers advanced technologies

Received: 15 February 2010, Revised: 24 March 2010, Accepted: 24 March 2010, Published online in Wiley Online Library: 18 June 2010

(wileyonlinelibrary.com) DOI: 10.1002/pat.1731

Development of PEGylated doxorubicin-E-[c(RGDfK)$_2$] conjugate for integrin-targeted cancer therapy

Dina Polyak[a], Claudia Ryppa[b], Anat Eldar-Boock[a], Paula Ofek[a], Ariel Many[c], Kai Licha[d], Felix Kratz[b] and Ronit Satchi-Fainaro[a]*

Doxorubicin (DOX) is extensively used in cancer therapy; however, it is cardiotoxic in cumulative doses and chemoresistance can evolve with prolonged use. Conjugation of a chemotherapeutic agent to a water-soluble polymeric carrier prolongs the circulation life of the drug, promotes its accumulation at the tumor site due to the enhanced permeability and retention (EPR) effect and prevents the drug from extravasating into healthy tissues. We designed and synthesized a delivery system that enables the conjugation of a targeting moiety, Arg-Gly-Asp (RGD) peptidomimetic, on one end of a linear poly(ethylene glycol) (PEG) chain, and DOX on the other end. The drug was bound to the polymer through an acid-sensitive (6-maleimidocaproyl)hydrazone linker. The resulting PEG-DOX-E-[c(RGDfK)$_2$] conjugate actively and selectively targets endothelial and tumor cells overexpressing $\alpha_v\beta_3$ integrin. Alternatively, we conjugated the PEG-DOX with a control c(RADfK) peptide that does not bind to $\alpha_v\beta_3$ integrin, resulting in a PEG-DOX-c(RADfK) conjugate. The PEG-DOX-E-[c(RGDfK)$_2$] conjugate and free DOX exhibited similar cytotoxic effect on U87-MG human glioblastoma cells. Interestingly, treatment with the conjugate inhibited the proliferation of DOX-resistant M109 murine lung carcinoma cells at a lower IC$_{50}$ compared with free DOX and PEG-DOX-c(RADfK). In addition, PEG-DOX-E-[c(RGDfK)$_2$] inhibited the proliferation of human umbilical vein endothelial cells and their attachment to fibrinogen-coated wells. Preliminary *in vivo* near-infrared studies revealed that a PEG-E-[c(RGDfK)$_2$]-cyanine conjugate preferentially accumulated in mCherry-labeled-DA3 murine mammary tumors inoculated orthotopically in female BALB/c mice. Altogether, our results show a proof of principle for a selective delivery of DOX to endothelial and cancer cells overexpressing $\alpha_v\beta_3$ integrin. Copyright © 2010 John Wiley & Sons, Ltd.

Supporting information may be found in the online version of this paper.

Keywords: tumor angiogenesis; $\alpha_v\beta_3$ integrin; polymer therapeutics; doxorubicin; poly(ethylene glycol)

INTRODUCTION

Anthracyclines rank among the most effective anticancer drugs ever developed in terms of response rates, remission duration, and survival,[1–4] with a broad spectrum of activity in a variety of human cancers.[5] They act by stabilizing a reaction intermediate in which DNA strands are broken and covalently linked to tyrosine residues of topoisomerase II, eventually impeding DNA resealing. Topoisomerase II-mediated DNA damage is followed by growth arrest in G1 and G2 and programmed cell death.[6] Doxorubicin (DOX), one of the first anthracyclines isolated in the 1960s, is an essential component in the treatment of breast cancer, childhood solid tumors, soft tissue sarcomas, and aggressive lymphomas.[7] However, its clinical use is restricted by tumor resistance and cumulative dose-related cardiotoxicity. Life-time cumulative dose over 500 mg/m^2 was associated with congestive heart failure (CHF) in patients, whereas DOX-induced cardiomyopathy was seen at lower doses in patients with risk factors such as age, myocardial heart disease and hypertension.[8] Although the exact mechanism of cardiotoxicity is unknown, it has been shown that free radicals generated by DOX are involved.[9]

* *Correspondence to: R. Satchi-Fainaro, Department of Physiology and Pharmacology, Sackler School of Medicine, Room 607, Tel Aviv University, Tel Aviv 69978, Israel.*

a *D. Polyak, A. Eldar-Boock, P. Ofek, R. Satchi-Fainaro*
Department of Physiology and Pharmacology, Sackler School of Medicine, Room 607, Tel Aviv University, Tel Aviv 69978, Israel

b *C. Ryppa, F. Kratz*
Tumor Biology Center, Breisacher Strasse 117, 79106 Freiburg, Germany

c *A. Many*
Lis Maternity Hospital, Sourasky Medical Center, Tel Aviv, Israel

d *K. Licha*
mivenion GmbH, Robert-Koch-Platz 4, 10115 Berlin, Germany

Contract/grant sponsor: The Israel Science Foundation; contract/grant number: 1300/06.
Contract/grant sponsor: United States-Israel Binational Science Foundation; contract/grant number: 2007347.
Contract/grant sponsor: Recanati Fund for Medical Research (Tel Aviv University).
Contract/grant sponsor: Israel Cancer Association.
Contract/grant sponsor: Igal Alon Foundation (RSF).
Contract/grant sponsor: Dr Mildred Scheel Stiftung der Deutschen Krebshilfe.

Several approaches have been used to reduce the incidence of the cardiac toxicity of anthracyclines. These include dose limitation, close cardiac monitoring, alteration of dosing schedules, development of new anthracycline analogs, and administration of protective agents. In addition, various drug delivery systems were developed in an effort to improve the therapeutic index of conventional DOX chemotherapy.[9–11]

The main approaches used include: (a) polymer-drug conjugates (e.g. HPMA copolymer-DOX (PK1)),[12] (b) liposomal encapsulation (D-99, Myocet™),[13,14] PEGylated liposomal doxorubicin (Doxil®),[15] and (c) prodrugs (e.g. INNO-206).[16] Generally, these agents exhibited efficacies comparable to those of conventional DOX, with better safety profiles and less cardiotoxicity, although they still caused some other toxicities.[17] The delivery strategy of these vectors is based on the enhanced permeability and retention (EPR) effect: the circulating macromolecular drug delivery system extravasates from the leaky tumor vasculature and accumulates in the tumor due to the abnormal lymphatic drainage.[18,19]

Angiogenesis, the formation of new blood vessels from pre-existing ones, is now recognized as an important control point in cancer therapy.[20–22] Tumor endothelial cells are drug sensitive for long periods of time and may be treated with cytotoxic agents in a metronomic schedule, which involves the administration of chemotherapy at low doses and in close intervals for extended periods of time.[23] As a result, acute toxicity should be avoided and the drugs may be administered for longer periods to exert their effect on the tumor endothelial cells and not the tumor cells directly.[24] Tumor neovascularization is a highly regulated process that depends on coordinated signaling of growth factors and cell adhesion receptors.[20] Tumor endothelial associated molecules, preferentially expressed during angiogenesis, can be successfully targeted by anti-angiogenic and anti-tumor therapeutics.[25,26] Several small molecules and macromolecular conjugates with diagnostic or therapeutic agents have been developed for targeting the tumor vasculature.[27]

$\alpha_v\beta_3$ integrin is one of the molecular markers that distinguish newly formed capillaries from their mature counterparts. Integrins are a class of receptors involved in the mechanism of cell adhesion to the extracellular matrix (ECM).[28] They play an important role in transferring signals from the extracellular environment to the intracellular compartment. Although endothelial cells express many different integrins, $\alpha_v\beta_3$ appears to be the most significant for angiogenesis.[29] This integrin is highly expressed on activated endothelial cells and newborn vessels, but is absent in resting endothelial cells and most normal organ systems, rendering it a suitable target for anti-angiogenic cancer therapy. In addition, it is also expressed on some tumor cells, allowing for both tumor cell and tumor vasculature targeted therapy.[29–31] Moreover, tumor progression, invasion and metastasis of breast cancer, glioma, melanoma, and ovarian carcinoma are linked to $\alpha_v\beta_3$ integrin overexpression.[31–35] $\alpha_v\beta_3$ integrin binds the Arg-Gly-Asp (RGD) sequence which constitutes the recognition domain of different ECM components such as laminin, fibronectin, and vitronectin. Inhibition of $\alpha_v\beta_3$ integrin activity by cyclic RGD peptide antagonists has been shown to induce endothelial cell apoptosis and to inhibit angiogenesis.[36,37]

In this report we PEGylated DOX and linked it to E-[c(RGDfK)$_2$], an $\alpha_v\beta_3$ integrin specific binding moiety. Diagnostic studies by Janssen *et al.* have demonstrated that this bis-cyclic form of c(RGDfK) i.e. E-[c(RGDfK)$_2$] has improved tumor targeting properties over the monomeric form.[38,39] Subsequent biodistribution studies with radiolabeled E-[c(RGDfK)$_2$] showed an uptake of up to 7.5% injected dose/g in human ovarian OVCAR-3 xenograft tumors.[39]

Poly(ethylene glycol) (PEG) is a linear or branched polyether terminated with hydroxyl groups.[40] It is a water-soluble, biocompatible, non-toxic, clinically approved and non-immunogenic polymeric carrier.[41] Our novel conjugate combines passive targeting to the tumor site (by the EPR effect) with active targeting to proliferating endothelial and cancer cells which overexpress $\alpha_v\beta_3$ integrin (by RGD peptidomimetic (PM)). By this approach, we aimed to deliver DOX selectively to the tumor tissue thus minimizing its side effects. As controls we synthesized and investigated analogously constructed DOX-PEG conjugates without an RGD moiety and an additional one containing the scrambled sequence c(RADfK) that does not bind $\alpha_v\beta_3$ integrin.

MATERIALS AND INSTRUMENTAL

Doxorubicin hydrochloride (*Mr* 579.98 g/mol) was purchased from Yick-Vic, (Hong Kong, PRC). The (6-maleimidocaproyl) hydrazone derivative of doxorubicin (DOX-EMCH • HCl) was synthesized as described previously [16]; E-[c(RGDfK)$_2$] (Fig. 1SA) and c(RADfK) (Fig. 1SB) were purchased from Peptides International (Louisville, KY, USA); Trt-S-C_2H_4-NHCO-PEG-C_3H_6COO-NHS (M_W 11.7 kDa) and Trt-S-C_2H_4-NHCO-PEG-C_3H_6COOH (M_W 11.6 kDa) was purchased from Rapp Polymers (Germany). The maleimide derivative of the indotricarbocyanine TSCA-mal was provided by mivenion GmbH, Germany (Fig. 1SC). Organic solvents were HPLC grade (Labscan Ltd, Dublin, Ireland; Roth, Karlsruhe, FRG; Merck, Darmstadt, Germany). All other chemicals used were at least reagent grade and obtained from Sigma-Aldrich (Deisenhofen, Germany) or Merck (Darmstadt, Germany) and used without further purification; buffers were vacuum-filtered through a 0.2 μm membrane (Sartorius, Germany) and thoroughly degassed with nitrogen prior to use. Mass spectra were obtained on a Thermo Electron LCQ Advantage with associated MAT SS 200 data system using electron spray ionization. UV/VIS-spectrophotometry was carried out with a double-beam spectrophotometer U-2000 from Hitachi. Analytical HPLC for the indotricarbocyanine dye PEG conjugates were performed with a Gilson 321 pump, a Kontron 535 detector (at 758 nm) and a Bischoff Lambda 1010 detector (at 220 nm). For peak integration Geminyx software (version 1.91 by Goebel Instrumentelle Analytik, Germany) was used; column: BioSil SEC250 (300 × 7.8 nm with a pre-column from BioRad, Germany; flow); 1.2 ml/min, mobile phase: 10% can, 90% 4 mM sodium phosphate buffer containing 0.15 M NaCl, pH 7.0); injection volume: 50 μl.

HPLC for the determination of the purity of the PEG-DOX conjugates was performed on a Waters system (pump: Waters 616, detector: Waters 996 photodiode array detector; controller: Waters 600S; autosampler: Waters 717; software: Empower 2002); chromatographic conditions: Waters Symmetry® C18 column (300-5, 250 × 4.6 mm) with pre-column; chromatographic conditions: flow: 1.0 ml/min; mobile phase A: 25% MeCN, 75% 10 mM potassium phosphate; mobile phase B: 70% MeCN, 30% 10 mM potassium phosphate; gradient: 0–26 min 100% mobile phase A; 0–15 min 0–100% mobile phase A; 15–35 min 100% mobile phase

B isocrat.; 35–40 min 100% mobile phase B; 40–60 min 100% mobile phase A; injection volume: 50 μl.

EBM-2 and EGM-2 medium were from Lonza, Switzerland and endothelial cells growth supplement (ECGS) from Zotal, Israel. All other tissue culture reagents were of general laboratory grade and were purchased from Biological Industries Ltd (Beit Haemek, Israel), unless otherwise stated.

Cell culture

U87-MG human glioblastoma and MCF-7 human metastatic breast cancer cells were obtained from the American Type Culture Collection (ATCC). Murine mammary adenocarcinoma DA3 cells were derived from the D1-DMBA-3 transplantable mammary tumor and obtained from the laboratory of I. Keydar (Tel Aviv University, Israel) through the courtesy of I. Tsarfaty (Tel Aviv University) and grown as previously described.[15,42] Cells were cultured in Dulbecco's modified Eagle's medium (DMEM) supplemented with 10% FBS, 100 U/ml Penicillin, 100 μg/ml Streptomycin, 12.5 U/ml Nystatin and 2 mM L-glutamine. Human umbilical vein endothelial cells (HUVEC) were isolated in our laboratory as previously described[43] and cultured in EGM-2 medium. Umbilical cords were collected at Lis Maternity Hospital, Sourasky Medical Center, Tel Aviv, Israel. The protocol was approved by the Institutional Review Board (IRB). All cells were grown at 37°C in 5% CO_2. DOX-sensitive-M109 murine lung carcinoma (M109S) cells and a subline of these cells, M109R, displaying multidrug resistance (an approximately 100-fold increased resistance to DOX) were obtained from BALB/c mice.[44] M109S and M109R cells, kindly provided by A. Gabizon (Shaare Zedek Medical Center Jerusalem) were cultured in RPMI medium supplemented with 10% FBS, 100 U/ml Penicillin, 100 μg/ml Streptomycin and 2 mM L-glutamine and grown at 37°C in 8% CO_2.

METHODS

Ethics statement

All animal procedures were performed in compliance with Tel Aviv University, Sackler School of Medicine guidelines and protocols approved by the Institutional Animal Care and Use Committee. Body weight and tumor size were monitored daily.

Establishment of mCherry-infected DA3 murine breast adenocarcinoma cell line

HEK 293T cells were transfected with pQC-mCherry, and the compatible packaging plasmids (pGag-pol.gpt and VSVG). The infecting retroviral particles were produced as previously described.[45] DA3 cells were infected with pQC-mCherry retroviral particles, and 48 hr following the infection, mCherry positive cells were selected by puromycin resistance. The infected cell line was named DA3-mCherry.

Conjugation of PEG with an E-[c(RGDfK)$_2$] moiety

N,N-Diisopropylethylamine (DIEA) (10.2 ml, 59.8 mmol, 1 equiv.) was added to a solution of the Trt-S-C_2H_4-NHCO-PEG-C_3H_6COO-NHS (700 mg, 59.8 mmol, 1 equiv.) and E-[c(RGDfK)$_2$] (78.9 mg, 59.8 mmol, 1 equiv.) in dry dimethylformamide (DMF) (15 ml). The solution was stirred at room temperature for 48 hr, then, precipitated in dry diethyl ether (300 ml), washed with pentane (150 ml), filtered and dried *in vacuo* to obtain a white powder in 89% yield (694 mg, 53.4 mmol). The material was stored at −20°C. The protected Trt-S-PEG-E-[c(RGDfK)$_2$] (25 mg) in 400 μl TFA/DCM 1:1 v/v (containing 2.5% *i*Pr_3SiH, 5% thioanisole/anisole, 1:1 v/v; 5% H_2O) was sonicated for 30–60 sec (clear yellow solution turned into clear colorless solution) and then stirred at room temperature for 20 min. The solvent was removed in high vacuum (approximately 20 min). Petrol ether/ether (1.5–2 ml, 1:1 v/v) was added to the residue and sonicated for approximately 30 sec. The supernatant was removed after centrifugation and dry ether was added to the residue and it was dissolved in 500 μl 50 mM sodium phosphate buffer pH 7. The pH of the remaining solution (470 μl) was adjusted to 7–7.5 with 0.1 N NaOH. The amount of SH groups was determined with Ellman (3×10 μl solution; 412 nm, $\lambda = 13{,}600\ M^{-1}\ cm^{-1}$). The solution was used directly for the coupling to the maleimide-bearing DOX derivatives.

Conjugation of PEG with a c(RADfK) moiety

DIEA (24 μl, 16.2 μmol, 1 equiv.) was added to a solution of the RAPP-PEG (154 mg, 16.2 μmol, 1 equiv.) and c(RADfK) (10 mg, 16.2 μmol, 1 equiv.) in dry DMF (1 ml). The solution was stirred at room temperature for 48 hr, then precipitated in dry diethyl ether (20 ml), washed with pentane (20 ml), filtered and dried *in vacuo* to obtain a white powder in 89% yield (103 mg, 16 μmol). The material was stored at −20°C. The protected Trt-S-PEG-c(RADfK) (25 mg) in 400 μl TFA/DCM 1:1 v/v (containing 2.5% *i*Pr_3SiH, 5% thioanisole/anisole, 1:1 v/v; 5% H_2O) was sonicated for approximately 30 sec (clear yellow solution turned into clear colorless solution) and stirred at room temperature for 20 min. The solvent was removed in high vacuum (approximately 20 min). Petrol ether/ether (1.5–2 ml, 1:1 v/v) was added to the residue and sonicated for ∼30 sec. The supernatant was removed after centrifugation, dry ether was added to the residue and it was dissolved in 500 μl 50 mM sodium phosphate buffer pH 7. The pH of the remaining solution (470 μl) was adjusted to 7–7.5 with 0.1 N NaOH. The amount of SH groups was determined with Ellman (3×10 μl solution; 412 nm, $\lambda = 13{,}600\ M^{-1}\ cm^{-1}$). The solution was used directly for the coupling to the maleimide-bearing DOX derivatives.

Synthesis of PEG-DOX-EMCH

The amount of SH groups of a solution of the Rapp-PEG in 50 mM sodium phosphate buffer pH 7 (20 mg/500 μl buffer) was determined (3-fold determination, $\lambda = 412$ nm; $\varepsilon = 13{,}600\ M^{-1}\ cm^{-1}$). DOX-EMCH • HCl (1.25 equiv., 25 mM stock solution: 20 mg/1 ml 10 mM sodium phosphate buffer; containing 0.6% *N*-acetyltryptophane; pH 6) was added to a solution of the Rapp-PEG dissolved in 50 mM sodium phosphate buffer (containing 0.6% *N*-acetyltryptophane) pH 7. The red solution was sonicated for approximately 30 sec and stirred on ice for 4 hr. The solution was applied to column chromatography on G 25 Sephadex with 10 mM sodium phosphate buffer pH 7 (containing 5% glucose) while the eluate was kept on ice. Then, it was adjusted to a concentration of approximately 300 μM by adding 10 mM sodium phosphate buffer pH 7 (containing 5% glucose) and the final concentration was determined by photometry (3-fold determination, $\lambda = 495$ nm, $\varepsilon_{DOX\text{-}EMCH} = 9250\ M^{-1}\ cm^{-1}$). Samples were aliquoted and stored at −80°C.

Conjugation of HS-PEG-c(RADfK) with DOX-EMCH

(6-maleimidocaproylhydrazone) derivative of DOX (DOX-EMCH • HCl) (1.25 equiv., 25 mM stock solution: 20 mg/1 ml 10 mM sodium phosphate buffer; containing 0.6% *N*-acetyltryptophane; pH 6) was added to a solution of HS-PEG-c(RADfK) dissolved in 50 mM sodium phosphate buffer (containing 0.6% *N*-DL-acetyltryptophane), pH 7. The red solution was sonicated for ~30 sec and stirred on ice for 4 hr, and then applied to column chromatography on G 25 Sephadex with 10 mM sodium phosphate buffer pH 7 (containing 5% glucose) and the fractions collected kept on ice. Purity of the solution was determined by analytical C-18-HPLC at 495 nm.

Conjugation of HS-PEG-E-[c(RGDfK)$_2$] with DOX-EMCH

(6-maleimidocaproylhydrazone) derivative of DOX (DOX-EMCH • HCl) (1.25 equiv., 25 mM stock solution: 20 mg/1 ml 10 mM sodium phosphate buffer; containing 0.6% *N*-acetyltryptophane; pH 6) was added to a solution of HS-PEG-E-[c(RGDfK)$_2$] dissolved in 50 mM sodium phosphate buffer (containing 0.6% *N*-DL-acetyltryptophane) pH 7. The red solution was sonicated for approximately 30 sec and stirred on ice for 4 hr. The PEG conjugate was isolated by column chromatography on G 25 Sephadex with 10 mM sodium phosphate buffer pH 7 (containing 5% glucose) with the fractions being kept on ice. The yield of the conjugate was determined by photometry (3-fold determination, $\lambda = 495$ nm; $\varepsilon_{\text{DOX-EMCH}} = 9250\ M^{-1}\,cm^{-1}$). Purity of the solution was determined by analytical C-18-HPLC at 495 nm.

Flow cytometric evaluation of $\alpha_v\beta_3$ integrin expression

The specific surface expression of $\alpha_v\beta_3$ was determined by flow cytometry using a MAB1976-anti-$\alpha_v\beta_3$ integrin antibody (clone LM609; Chemicon International). HUVEC and U87-MG cells were washed and then harvested in cold PBS (containing Mg^{2+} and Ca^{2+}). Cells were pelleted and re-suspended in serum-free medium followed by 30 min incubation. 1×10^6 cells/ml were then pelleted and incubated for 30 min at RT with the anti-$\alpha_v\beta_3$ integrin antibody (1:20). Control samples were incubated in the absence of the antibody. Cells were then washed twice, re-suspended in cold PBS, and incubated with a fluorescein isothiocyanate (FITC)-conjugated anti-mouse IgG secondary antibody (1:50, Jackson Immunoresearch Laboratories, West Grove, PA, USA) for 30 min at RT. Finally, cells were washed, re-suspended in PBS and separated using a 100 μm cell strainer (BD Biosciences, Bedford, MA, USA). Flow cytometry analysis was performed with a fluorescence-activated cell sorter (FACS) (6Cytek DxP 6-Color Upgrade, Facscan™). Statistical analysis was performed using WinMDI software.

Semi-quantitive RT-PCR

Total RNA extraction from several cancer cell lines was performed using the "EZ-RNA" kit (Biological Industries, Israel) according to the manufacturer's instructions. The Reverse Transcriptase reaction was performed with the "EZ-first strand cDNA synthesis kit" (Biological Industries, Israel) using oligo(dT) primers. PCR reactions were carried out using PCR-ReadyTM High Specificity (Syntezza) in an ATC 401 thermocycler (Apollo, CLP). To obtain semi-quantitative results, the number of cycles for each reaction was calibrated and kept to a minimum.

PCR primers: Human β_3 Integrin: 5′-AAGCACTGGGTGGT-GATTG-3′, 5′-TGAGGTCAAGGTGTGTGA-3′; Murine β_3 Integrin: 5′-AAGCACTGGGTGGTGATTG-3′, 5′-TGAGGTCAAGGTGTGTGA-3′; GAPDH (Human and mouse): 5′-CCATCACCATCTTCCAGGAGC-3′, 5′-GGCATGGACTGTGGTCATGAG-3′.

Cell viability assay

HUVEC were plated at 15,000 cells/well onto 24-well culture plates. Human glioblastoma U87-MG cells were plated at 3000 cells/well onto 96-well culture plates. Murine lung carcinoma M109S and M109R cells were plated at 4000 cells/well onto 96-well culture plates. After 24 hr, cells were exposed to several treatments at serial concentrations for 72 hr. All concentrations of PEG-DOX-E-[c(RGDfK)$_2$] conjugates used in the experiments are expressed as DOX-equivalent dose.

Cell viability was assayed by a Z1 Coulter® Particle Counter (Beckman Coulter™) for HUVEC or using a modified 3-(4,5-dimethylthiazol-2-yl)-2,5-diphenyltetrazolinium bromide (MTT) assay. Cell survival assay was performed by addition of 25 μl of 3 mg/ml MTT solution in PBS to each well followed by 5 hr incubation. The medium was then discarded and 200 μl dimethyl sulfoxide (DMSO) were added to dissolve the formazan crystals formed. Absorbance was measured at 560 nm. Cell viability is evaluated by the determination of IC_{50}, the inhibitory concentration of DOX that kills 50% of the cells.

Endothelial and tumor cells viability assay—"Pulse and Chase" short exposure

Cell viability was evaluated as described above with the exception that the cells were exposed to the drugs for a shorter period of time. Cells were incubated with the tested drugs for 60 min, then washed and incubated with either DMEM (for U87-MG) or EGM-2 (for HUVEC) medium without any additional treatment for 36 hr. Following this procedure, cell viability was assayed as described in the previous section (Coulter Counter or MTT).

Cell internalization of PEG-DOX-E-[c(RGDfK)$_2$] compared with the internalization of PEG-DOX-c(RADfK)

U87-MG cells (1×10^6 cells/plate) were plated onto 6 mm culture plates. Following 24 hr incubation, cells were exposed to DOX, PEG-DOX-c(RADfK) and PEG-DOX-E-[c(RGDfK)$_2$] diluted in DMEM medium. Cells were exposed to the treatment for 5, 15, 30, 60, 180, 300, and 480 min, then washed in PBS (3×), harvested and analyzed with the ImageStream 100 (Amnis). Analysis was performed using IDEAS software.

Endothelial cell adhesion assay

The ability of free and PEG-conjugated E-[c(RGDfK)$_2$] to bind $\alpha_v\beta_3$ integrin on the cell surface was evaluated by HUVEC adherence to fibrinogen following incubation with the compounds. Flat bottom 96-well culture plates were coated with 0.5 μg/well fibrinogen (overnight, 4°C). Following three washes with PBS, the wells were blocked with 1% bovine serum albumin (BSA) for 1 hr at 37°C. HUVEC were harvested in PBS with 2.5 mM EDTA, re-suspended in EBM-2 serum-free media and were incubated with the different treatments for 30 min at RT. Treated HUVEC were then plated at 2.5×10^4 cells/well and allowed to attach to fibrinogen-coated plates for 1 hr at 37°C. Following incubation,

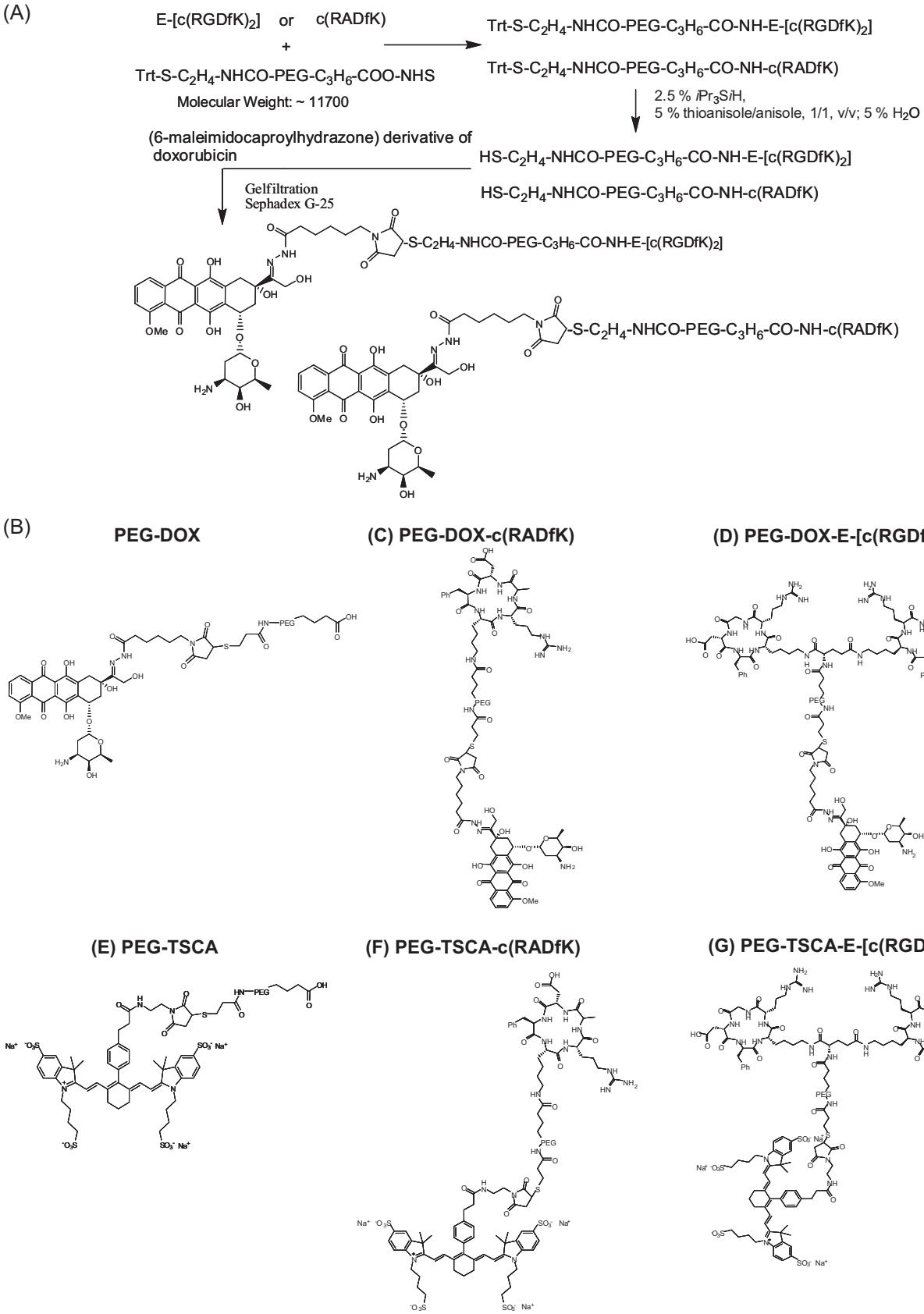

Figure 1. (A) Synthesis and (B–G) chemical structures of synthesized conjugates. (B) PEG-DOX, $M_W = 10{,}450$ g/mole; (C) PEG-DOX-c(RADfK) $M_W = 12{,}810$ g/mole; (D) PEG-DOX-E-[c(RGDfK)$_2$] $M_W = 13{,}510$ g/mole; (E) PEG-TSCA $M_W = 10{,}890$ g/mole; (F) PEG-TSCA-c(RADfK) $M_W = 13{,}250$ g/mole and (G) PEG-TSCA-E-[c(RGDfK)$_2$] $M_W = 13{,}950$ g/mole.

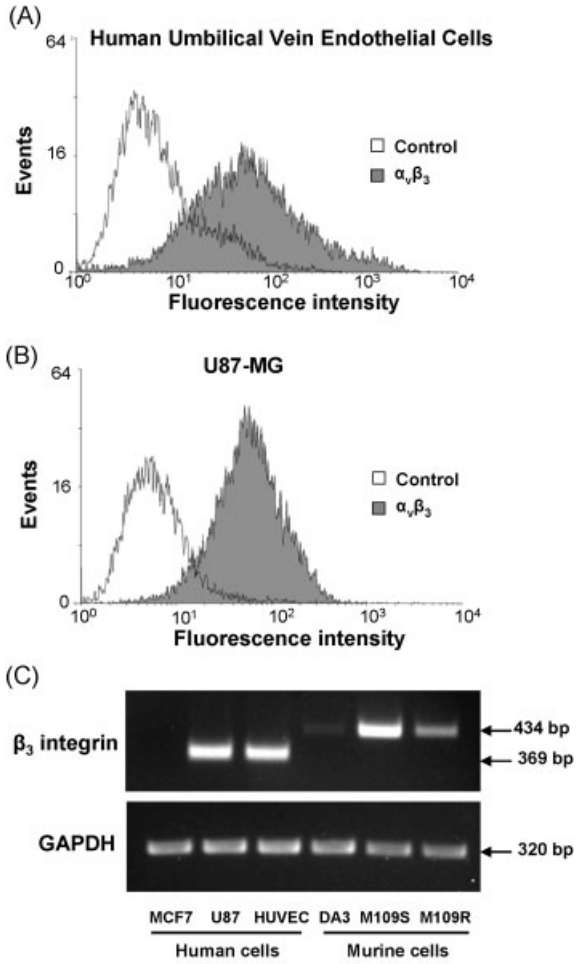

Figure 2. αvβ3 Integrin expression in human and murine cell lines. FACS evaluation of $\alpha_v\beta_3$ integrin expression in (A) HUVEC and (B) U87-MG cells. The specific surface expression of $\alpha_v\beta_3$ in HUVEC and U87-MG cells was determined by flow cytometry by measuring the binding of a mouse anti-$\alpha_v\beta_3$ antibody (clone LM609; Chemicon). (C) Total RNA was isolated from several cancer cell lines: human MCF-7, U87-MG and HUVEC; murine DA3, M109S and M109R. β_3 integrin mRNA levels were monitored and calibrated to GAPDH mRNA levels (semi-quantitive RT-PCR). HUVEC, M109S and U87-MG cells expressed high levels of β_3 integrin, while M109R and DA3 expressed lower levels. MCF-7 did not express β_3 integrin.

unattached cells were removed by rinsing the wells with PBS. Attached cells were fixed with 3.7% formaldehyde, stained with 0.5% crystal violet and imaged using a Nikon TE2000E inverted microscope integrated with a Nikon DS5 cooled CCD camera by 6× objective, bright field technique. The number of attached cells was quantified with NIH ImageJ processing and analysis software. Non-specific binding was determined by adhesion to BSA-coated plates.

In vivo assessment of the biodistribution of near-infrared fluorescent PEG-cyanine dye conjugates

BALB/c female mice were inoculated orthotopically with 1×10^6 mCherry-labeled-DA3 mammary adenocarcinoma cells. Tumor bearing-mice were injected intravenously with PEG-TSCA, PEG-TSCA-c(RADfK) or PEG-TSCA-E-[c(RGDfK)$_2$] (0.5 μmol/kg, $n = 3$ mice per group, average tumor weight = 140, 84, and 93 mg, respectively). Three hours later, mice were euthanized; tumors and selected organs were dissected, weighed and analyzed by CRI Maestro™ non-invasive fluorescence imaging system.

CRI Maestro™ non-invasive fluorescence imaging system was used to follow tumor progression of mCherry-labeled-DA3 mammary tumors and for accumulation studies of PEG-TSCA, PEG-TSCA-c(RADfK) or PEG-TSCA-E-[c(RGDfK)$_2$] conjugates. Mice were anesthetized using ketamine (100 mg/kg) and xylazine (12 mg/kg), treated with a depilatory cream (Veet®) and placed inside the imaging system. Alternatively, selected organs from mice were dissected and placed inside the imaging system. Multispectral image-cubes were acquired through 550–900 nm spectral range in 10 nm steps using excitation (595 nm for mCherry and 704 nm for near-infrared dye) and emission (645 nm for mCherry and 750 nm for near-infrared dye, longpass) filter set. Mice autofluorescence and undesired background signals were eliminated by spectral analysis and the Maestro™ linear unmixing algorithm.

RESULTS AND DISCUSSION

Chemistry

The PEG conjugates with E-[cRGDfK)$_2$] or c(RADfK) and the (6-maleimidocaproylhydrazone) derivative of doxorubicin (DOX-EMCH) were prepared as described in Fig. 1(A).

PEG-DOX-EMCH was synthesized by direct coupling of DOX-EMCH to commercially available HS-C_2H_4-CONH-PEG-C_3H_6-COOH (10 kDa) and isolating the conjugate through size-exclusion chromatography (Sephadex G-25). The purity of the three PEG-DOX conjugates (Fig. 1B–D) was determined by analytical reverse HPLC (C-18) and resulted in >98% at 495 nm (peaks for the respective conjugate eluting between 23 and 26 min). Control conjugates bearing no DOX were also synthesized.

The near-infrared PEG conjugates with tetrasulfoindotricarbocyanine-aryl-maleimide (TSCA-mal) (Fig. 1SC) were prepared in analogy to the PEG-DOX conjugates with the only difference that after conjugation with the thiol group, the conjugates were isolated with Sephacryl S100. To determine the amount of dye present in the PEG conjugate, an ε-value of 390,000 M^{-1} cm^{-1} based on TSCA at 758 nm was used (in 10 mM sodium phosphate/5% glucose buffer, pH 7.0). Purity of the PEG conjugates was determined on an HPLC size-exclusion column (BioSil SEC250) and were isolated with a purity of 93–96% at 220 nm showing absence of free dye after gel filtration and a peak at all conjugates eluted between 15.0 and 16.0 min for the respective PEG-dye-conjugate.

Accordingly, the conjugates PEG-TSCA, PEG-TSCA-c(RADfK), and PEG-TSCA-E-[c(RGDfK)$_2$] were prepared for comparative *in vivo* imaging studies (Fig. 1E–G).

Evaluation of $\alpha_v\beta_3$ Integrin expression in human and murine cell lines

To evaluate the interaction between E-[c(RGDfK)$_2$] and the $\alpha_v\beta_3$ integrin receptor, we first determined the expression levels of the $\alpha_v\beta_3$ integrin in several cell types using FACS. We found that human $\alpha_v\beta_3$ integrin is highly expressed on HUVEC and U87-MG cells (Fig. 2A–B). We further performed a semi-quantitive RT-PCR in order to characterize $\alpha_v\beta_3$ integrin expression in murine cells

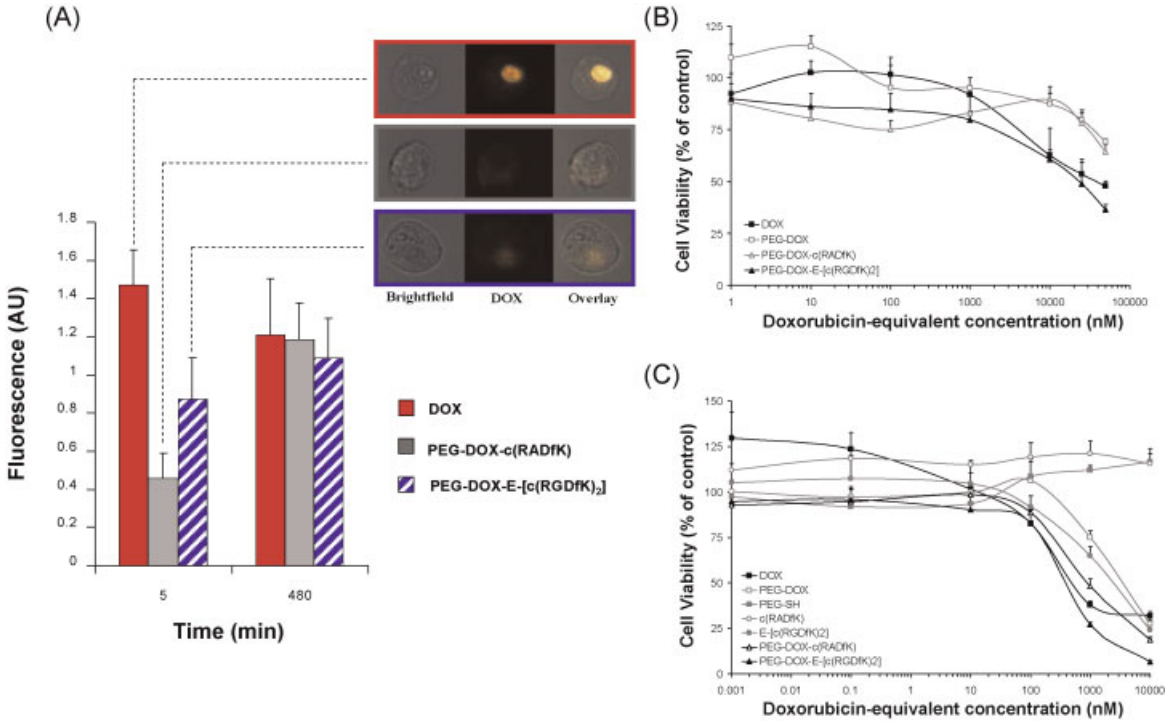

Figure 3. PEG-DOX-E-[c(RGDfK)$_2$] binds to U87-MG αvβ3 integrin overexpressing cells, internalizes and decreases their viability. The interaction between E-[c(RGDfK)$_2$] and the $\alpha_v\beta_3$ integrin on U87-MG cell was followed with an ImageStream® 100 Imaging Flow Cytometer (Amnis) (A) Free DOX (red) fully internalized in U87-MG cells following 5 min exposure, whereas this short exposure time was sufficient to show 2-fold increase in internalization of PEG-DOX-E-[c(RGDfK)$_2$] conjugate compared with the level of internalization of PEG-DOX-c(RADfK). Eight hours (480 min) later, PEG-DOX-c(RADfK) (gray), PEG-DOX-E-[c(RGDfK)$_2$] (blue stripes) and free DOX (red) were similarly internalized. Fluorescence is expressed in arbitrary units (AU). Data represent mean + variance parameter. (B) U87-MG cells were treated with PEG-DOX-E-[c(RGDfK)$_2$] (black triangles), PEG-DOX-c(RADfK) (white triangles), PEG-DOX (white squares) or free DOX (black squares) for 60 min. Thirty six hours post-incubation without the compounds, PEG-DOX-E-[c(RGDfK)$_2$] exhibited similar cytotoxic effect as free DOX, while cells treated with PEG-DOX and PEG-DOX-c(RADfK) did not reach the IC_{50} at the tested concentrations. (C) U87-MG cells were treated with PEG-DOX-E-[c(RGDfK)$_2$] (black triangles), PEG-DOX-c(RADfK) (white triangles), PEG-DOX (white squares), free DOX (black squares), PEG-SH (gray squares), c(RADfK) (white circles), or E-[c(RGDfK)$_2$] (gray circles) for 72 hr. The viability of U87-MG cells was similarly decreased by free DOX, PEG-DOX-c(RADfK) and PEG-DOX-E-[c(RGDfK)$_2$]. *x*-axis is presented at a logarithmic scale. Data represent mean + standard deviation (SD). This figure is available in color online at wileyonlinelibrary.com/journal/pat

as well. Given that β_3 integrin is the limiting factor in the formation of the $\alpha_v\beta_3$ integrin receptor, we evaluated β_3 expression levels in several cell lines. β_3 rendered a band of 369 bp in the human cell lines (U87-MG, HUVEC) and a band of 434 bp in the murine cell lines (DA3, M109S, M109R) (Fig. 2C). The results obtained from the PCR reaction clearly reinforce the data from the FACS analysis: $\alpha_v\beta_3$ integrin is highly expressed on HUVEC and U87-MG cells and not in MCF7 cells (negative control). Moreover, we show variable levels of expression on DA3, M109S and M109R cells (Fig. 2C).

PEG-DOX-E-[c(RGDfK)$_2$] conjugate induces cytotoxicity in $\alpha_v\beta_3$ integrin-overexpressing U87-MG cells via rapid internalization

Using the Amnis ImageStream 100, we took advantage of the fluorescent properties of doxorubicin in order to follow the interaction between E-[c(RGDfK)$_2$] and the $\alpha_v\beta_3$ integrin. We compared the fluorescence of cells treated with PEG-DOX-E-[c(RGDfK)$_2$] to that of cells treated with PEG-DOX-c(RADfK), to asses the internalization profile of targeted DOX in $\alpha_v\beta_3$ overexpressing tested cells. U87-MG cells were exposed to DOX, PEG-DOX-c(RADfK) and PEG-DOX-E-[c(RGDfK)$_2$] for different exposure times (from 5 min to 8 hr), and then analyzed with the ImageStream® 100 Imaging Flow Cytometer. Free DOX internalized into the cells following a short 5 min exposure and showed the same internalization profile for as long as 8 hr (Fig. 2S). Following 5 min of incubation of U87-MG cells with PEG-DOX-E-[c(RGDfk)$_2$], a 2-fold higher amount of the conjugate was internalized compared with PEG-DOX-c(RADfK) (Fig. 3A). The difference between the two conjugates was rapidly eliminated over time and after 15 min incubation, PEG-DOX-c(RADfK) and PEG-DOX-E-[c(RGDfK)$_2$] were internalized almost at a similar level (Fig. 2S). Eight hours following treatment, the level of internalized free DOX, PEG-DOX-c(RADfK) and PEG-DOX-E-[c(RGDfK)$_2$] were alike (Fig. 3A).

The $\alpha_v\beta_3$ integrin-overexpressing U87-MG cells, were exposed to DOX, PEG-DOX, PEG-DOX-c(RADfK), and PEG-DOX-E-[c(RGDfK)$_2$] at serial concentrations for 60 min, washed and further incubated for 36 hr (Fig. 3B). Cells treated with PEG-DOX-E-[c(RGDfK)$_2$] conjugate exhibited an IC_{50} of ~25 μM, while cells treated with PEG-DOX-c(RADfK) and PEG-DOX did not reach an IC_{50} even at 50 μM. Moreover, during short exposure times, targeted PEGylated DOX demonstrated similar cytotoxicity profile on $\alpha_v\beta_3$-expressing cells as the small molecule, free DOX.

Furthermore, we tested the cytotoxic effect of PEG-DOX-E-[c(RGDfK)$_2$] conjugate on U87-MG human glioblastoma

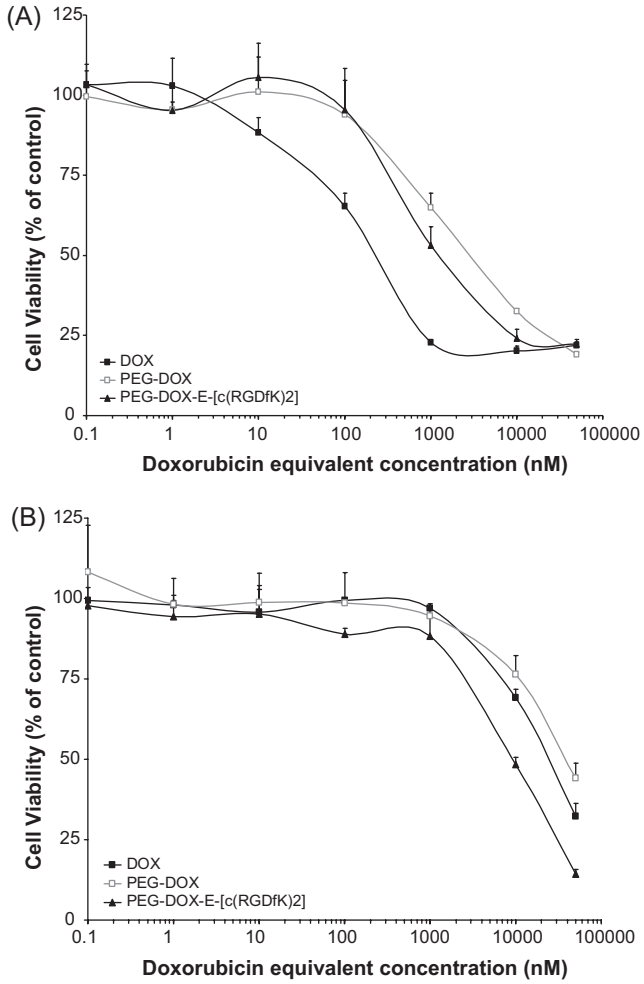

Figure 4. PEG-DOX-E-[c(RGDfK)$_2$] overcomes DOX resistance in M109R murine lung carcinoma cells. (A) M109S and (B) M109R cells were incubated with DOX (black squares), PEG-DOX (white squares) and PEG-DOX-E-[c(RGDfK)$_2$] conjugates (black triangles) for 72 hr. PEG-DOX and PEG-DOX-E-[c(RGDfK)$_2$] demonstrated a similar cytotoxic effect on M109S exhibiting an IC$_{50}$ of ~3 and ~1.2 μM, respectively. Free DOX exhibited a two orders of magnitude lower cytotoxic effect on M109R than on M109S cells, with an IC$_{50}$ of 25 μM. PEG-DOX-E-[c(RGDfK)$_2$] exhibited an IC$_{50}$ of 9 μM in M109R cells. *x*-axis is presented at a logarithmic scale. Data represent mean + SD.

cells under prolonged exposure (72 hr). Cells were treated with DOX, PEG-DOX, thiolated poly(ethylene glycol) (PEG-SH), E-[c(RGDfK)$_2$], c(RADfK), PEG-DOX-E-[c(RGDfK)$_2$] and PEG-DOX-c(RADfK) conjugates at serial concentrations for 72 hr (Fig. 3C and Fig. 3S showing the effect of the controls). The viability of U87-MG cells was inhibited similarly by free DOX, PEG-DOX-c(RADfK) and PEG-DOX-E-[c(RGDfK)$_2$] with an IC$_{50}$ of ~500 nM. These results can be easily explained by the fact that all the molecules will eventually enter the cell if enough time is given. The specifically targeted conjugates are in advantage following short exposure times, when only RGD-bound conjugates are able to bind the $\alpha_v\beta_3$ integrin receptor and rapidly enter the cell through receptor-mediated endocytosis.

PEG-DOX-E-[c(RGDfK)$_2$] conjugate overcomes resistance to DOX of M109R murine lung carcinoma cells

We tested the cytotoxic effect of PEG-DOX-E-[c(RGDfK)$_2$] conjugate on M109S (Fig. 4A) and M109R (Fig. 4B) murine lung carcinoma cells in order to determine whether our novel conjugate is able to overcome DOX resistance due to PEGylation and receptor mediated internalization. Cells were treated with DOX, PEG-DOX, and PEG-DOX-E-[c(RGDfK)$_2$] conjugates at serial concentrations for 72 hr.

M109S murine lung carcinoma cell viability was similarly inhibited by PEG-DOX and PEG-DOX-E-[c(RGDfK)$_2$] conjugates at DOX-equivalent concentration exhibiting an IC$_{50}$ of 3 and 1.2 μM, respectively. Free DOX by itself demonstrated an IC$_{50}$ value of ~250 nM (Fig. 4A). A different cytotoxicity pattern was seen in M109R cells which are resistant to DOX. Free DOX exhibited a two orders of magnitude lower cytotoxic effect on M109R than on M109S cells, with an IC$_{50}$ of 25 μM. However, PEG-DOX-E-[c(RGDfK)$_2$] partially overcame DOX resistance, exhibiting an IC$_{50}$ of 9 μM (Fig. 4B). These results suggest that our PEG-DOX-E-[c(RGDfK)$_2$] bypasses M109R cells' MDR pump, by delivering DOX into the cell via receptor-mediated endocytosis. All IC$_{50}$ values are summarized in Table 1.

PEG-DOX-E-[c(RGDfK)$_2$] conjugate is a potent anti-angiogenic inhibitor

Next, we wanted to evaluate the anti-angiogenic potential of PEG-DOX-E-[c(RGDfK)$_2$] because $\alpha_v\beta_3$ integrin is overexpressed on tumor endothelial cells (Fig. 2A, C). We assessed the effect of

Table 1. IC$_{50}$ values of all evaluated compounds on HUVEC, U87-MG human glioblastoma, M109S and M109R murine lung carcinoma cells

	IC50 values (nM)				
Compounds	HUVEC	U87-MG (36 hr)	U87-MG	M109S	M109R
Free DOX	6	40,000	500	250	25,000
PEG-DOX	80	>50,000	3500	3000	40,000
PEG-SH	3500	N/A	>10,000	N/A	N/A
c(RADfK)	>10,000	N/A	>10,000	N/A	N/A
E-[c(RGDfK)$_2$]	400	N/A	2500	N/A	N/A
PEG-DOX-c(RADfK)	50	>50,000	900	N/A	N/A
PEG-DOX-E-[c(RGDfK)$_2$]	40	25,000	400	1200	9000

The presented values were obtained from a 72 hours cell viability assay, unless otherwise stated.

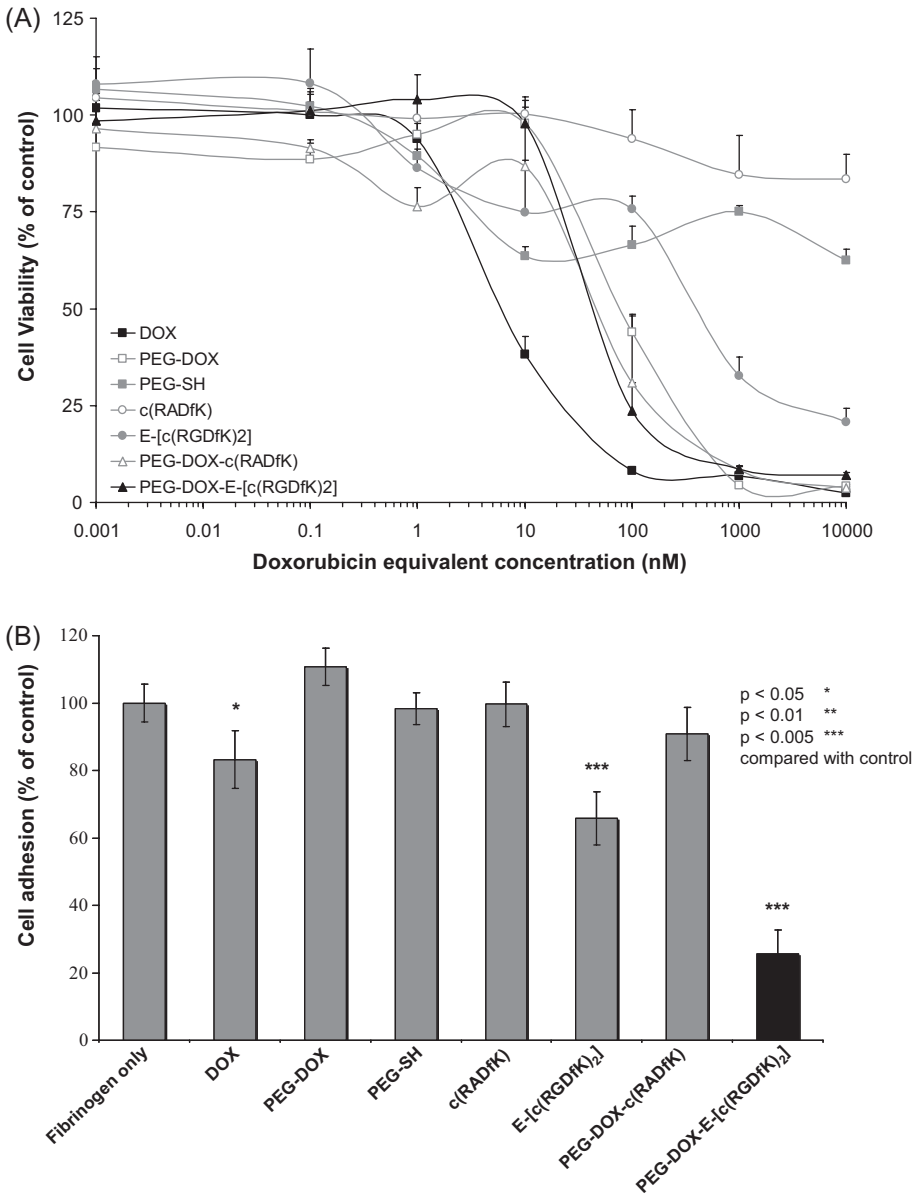

Figure 5. PEG-DOX-E-[c(RGDfK)$_2$] conjugate is a potent anti-angiogenic inhibitor. (A) HUVEC were incubated with DOX (black squares), PEG-SH (gray squares), E-[c(RGDfK)$_2$] (gray circles), c(RADfK) (white circles), PEG-DOX (white squares), PEG-DOX-E-[c(RGDfK)$_2$] (black triangles) and PEG-DOX-c(RADfK) (white triangles) conjugates for 72 hr. Cell viability was similar following treatment with PEG-DOX, PEG-DOX-c(RADfK) and PEG-DOX-E-[c(RGDfK)$_2$], ($IC_{50} \sim 50$ nM). Free DOX showed a more potent cytotoxic effect on HUVEC ($IC_{50} \sim 6$ nM). Drug concentrations are presented in nM, on a logarithmic scale. Data represent mean + SD. (B) Adhesion of HUVEC to fibrinogen was tested by incubation of the cells with DOX, PEG-SH, E-[c(RGDfK)$_2$] or c(RADfK), PEG-DOX-c(RADfK) or RGD-bearing PEG-DOX conjugates, at 50 μM DOX-equivalent concentration. PEG-DOX-E-[c(RGDfK)$_2$] (black) had an inhibitory effect of ~75% whereas PEG-DOX-c(RADfK) showed almost no inhibition (~10%). Data represent mean ± SD. $^{*}p < 0.05$, $^{**}p < 0.01$, $^{***}p < 0.005$ compared with control.

the conjugate on the proliferation of HUVEC. To do so, HUVEC were incubated with serial concentrations of PEG-DOX, PEG-DOX-E-[c(RGDfK)$_2$], and PEG-DOX-c(RADfK) conjugates. HUVEC were also treated with E-[c(RGDfK)$_2$], PEG-SH, and c(RADfK) for comparison.

HUVEC viability was inhibited by PEG-DOX, PEG-DOX-E-[c(RGDfK)$_2$], and PEG-DOX-c(RADfK) conjugates at a DOX-equivalent concentration exhibiting an IC_{50} of 80, 40, and 50 nM, respectively (Fig. 5A and Fig. 4S showing the effect of the controls). Free DOX exhibited higher HUVEC cytotoxicity demonstrating an IC_{50} value of ~6 nM, whereas PEG-SH and c(RADfK) peptide did not reach IC_{50} values at the tested concentrations. Interestingly, although expected, E-[c(RGDfK)$_2$] efficiently inhibited HUVEC proliferation exhibiting an IC_{50} of 400 nM. Furthermore, an endothelial cell adhesion assay was performed in order to evaluate the *in vitro* targeting specificity of the E-[c(RGDfK)$_2$] or c(RADfK) conjugated to PEGylated DOX. E-[c(RGDfK)$_2$] free or conjugated to DOX at equivalent concentrations of 50 μM inhibited HUVEC adhesion to fibrinogen (Fig. 5B). PEG-DOX-E-[c(RGDfK)$_2$] had an inhibitory effect of ~75% whereas PEG-DOX-c(RADfK) had almost no effect (~10%). Free E-[c(RGDfK)$_2$] served as control and exhibited an inhibitory effect

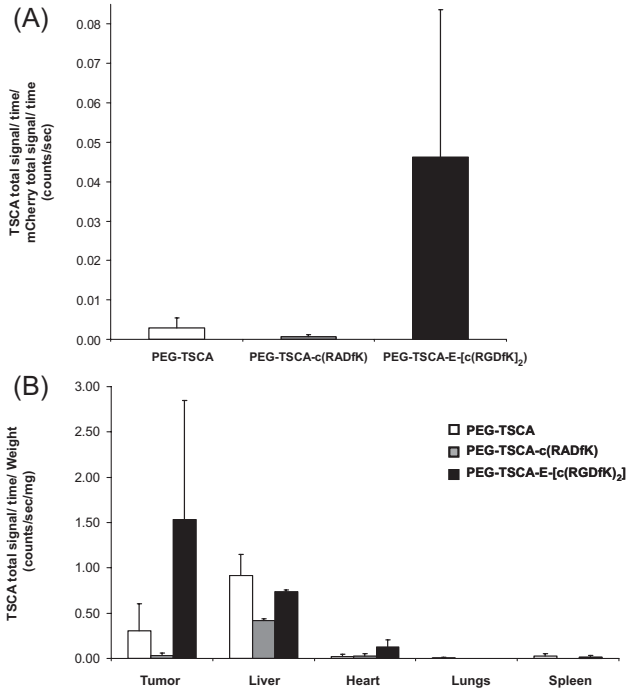

Figure 6. Biodistribution and tumor accumulation of PEG-TSCA conjugates in DA3-mCherry tumor-bearing BALB/c mice. (A) Accumulation of PEG-TSCA-E-[c(RGDfK)$_2$] (black), in a DA3 mammary tumor, was 15-fold and 7-fold higher than PEG-TSCA-c(RADfK) (gray) and PEG-TSCA (white) respectively. (B) Accumulation of PEG-TSCA-E-[c(RGDfK)$_2$] in a mammary tumor was much higher than in other selected organs ($n = 3$ mice per group). The fluorescent signal was followed by CRI Maestro™ non-invasive fluorescence imaging system. Data represent mean + standard error of the mean (SEM).

of ~35%, while c(RADfK), PEG-SH, and PEG-DOX had no effect on the adhesion of HUVEC to fibrinogen. These findings indicate a strong anti-angiogenic effect of PEG-DOX-E-[c(RGDfK)$_2$].

PEG-TSCA-E-[c(RGDfK)$_2$] conjugate accumulated selectively in DA3-mCherry tumors inoculated in BALB/c mice

Subsequently, we wanted to evaluate whether our conjugate is selectively targeted to and accumulated in DA3 mammary tumors due to the leaky vasculature and the $\alpha_v\beta_3$ integrin-overexpression on the endothelial cells (Fig. 2A, C).

Tumor specific accumulation of PEG-E-[c(RGDfK)$_2$] was evaluated using mCherry-labeled-DA3 mammary adenocarcinoma cells orthotopically inoculated in female BALB/c mice. The near infrared dye TSCA was PEGylated and conjugated to E-[c(RGDfK)$_2$] and used to evaluate PEG-DOX-E-[c(RGDfK)$_2$] biodistribution (Fig. 1E–G for structures). Mice were intravenously injected with PEG-TSCA, PEG-TSCA-c(RADfK), or PEG-TSCA-E-[c(RGDfK)$_2$]. Three hours following treatment, mice were euthanized; tumor and selected organs were dissected and imaged with CRI Maestro™ non-invasive fluorescence imaging system. Accumulation of PEG-TSCA-E-[c(RGDfK)$_2$] in mammary tumors was higher (0.046 counts/sec) than PEG-TSCA-c(RADfK) (0.0006 counts/sec) or PEG-TSCA (0.0028 counts/sec) (Fig. 6A). Additionally, PEG-TSCA-E-[c(RGDfK)$_2$] was selectively accumulated in the tumors rather than in other selected organs (Fig. 6B). Although DA3 cells did not show very high levels of $\alpha_v\beta_3$ integrin expression (Fig. 2C), the RGD-mediated targeting of the conjugate still worked very efficiently. Apparently the high levels of $\alpha_v\beta_3$ integrin expressed in tumor endothelial cells are enough to attract the PEG-DOX-E-[c(RGDfK)$_2$] conjugate even to a tumor expressing relatively low levels of the integrin.

CONCLUSIONS

Although both strategies of (i) targeting $\alpha_v\beta_3$ integrin and (ii) conjugation of DOX with a polymer are currently being evaluated in clinical trials, the thought of developing an anti-$\alpha_v\beta_3$ integrin and DOX bi-specific macromolecule targeting the tumor cells and their endothelial microenvironment had not been given previous consideration to date. Here we describe the design, synthesis and characterization of novel water-soluble PEG-DOX-RGD PM conjugates that target $\alpha_v\beta_3$ integrin overexpressed at the tumor site. The size of the obtained conjugates was around 13 kDa, thus having novel compounds in place which utilize the combination of passive and molecular targeting mechanisms.

Comparing the differently loaded conjugates and their anti-angiogenic activity on HUVEC by both adhesion and cytotoxicity assays showed an advantage for the bis-cyclic RGD bearing conjugates over the RAD PM, demonstrating greater adhesion to fibrinogen properties, as already presented.[35,46] In this study we further demonstrate that the conjugation of E-[c(RGDfK)$_2$] to PEG-DOX does not abrogate its inhibitory ability.

We further evaluated the anti-angiogenic and anticancer abilities of our novel conjugate showing it has a selectivity for $\alpha_v\beta_3$-integrin overexpressing cells, which were previously shown to attach RGD peptidomimetics,[47] either to inhibit them directly[48] or as targeting moieties.[17,35,46,49]

The anticancer activity of our conjugate was demonstrated, proving our hypothesis that it will have a clear advantage on $\alpha_v\beta_3$ integrin overxpressing cancer cell lines. We demonstrate that U87-MG human glioblastoma cells overexpress $\alpha_v\beta_3$ integrin and adhere to our E-[c(RGDfK)$_2$]-bearing conjugate. Consequently, the new conjugate not only targets U87-MG cells *in vitro*, but it also inhibits their viability.

More importantly, we showed that E-[c(RGDfK)$_2$] functions as a targeting moiety *in vivo*. Following intravenous injection, the conjugate travels in the vessels and passively extravasates at the tumor site because of the EPR effect, and it attaches to receptor-overexpressing cells. Our promising preliminary *in vivo* results, with near-infrared fluorescently labeled RGD-bearing PEG conjugate as basic model systems, are the beginning of the thorough endeavor we are presently undertaking.

A different class of drug delivery system bearing an $\alpha_v\beta_3$ integrin targeting moiety has been recently developed by Borgman *et al.*, consisting of HPMA copolymer-c(RGDfK)-aminohexylgeldanamycin (AH-GDM) conjugate bearing a cathepsin B-cleavable linker. The HPMA copolymer–c(RGDfK)–(AH-GDM) conjugate was tested *in vitro* showing cellular growth inhibition and cathepsin B-dependent drug release.[50] In addition, the integrin-targeting potential of these conjugates was tested *in vitro* and *in vivo* and was found to selectively accumulate in tumor tissue.[51] Here we describe a linear PEG polymer comprising of two active terminal groups, which were utilized to generate targeted PEG-DOX prodrug. The PEGylation of DOX and conjugation with E-[c(RGDfK)$_2$] did not affect its bioactivity, whereas the activity of geldanamycin was severely reduced as a result of its chemical modification to AH-GDM in

order to couple it to HPMA copolymer. Although HPMA copolymer–c(RGDfK)–(AH-GDM) conjugate showed decreased accumulation in other organs over time, large kidney accumulation was observed.[52]

Both the conjugation of a DOX with a PEG carrier and the addition of a targeting moiety were designed to alter and improve DOX efficacy and minimize its side effects. Another aspect that was challenged by this conjugation is overcoming DOX acquired resistance. DOX is an effective therapy for several cancer types; however, sensitivity to DOX varies among patients. The mechanism through which resistance develops is still unknown. In M109 murine lung carcinoma cancer cells, DOX resistance was developed. We tested whether the inhibitory effect of our PEG-DOX-E-[c(RGDfK)$_2$] conjugate on the proliferation of M109 cells differs from free DOX or PEG-DOX. Indeed PEG-DOX-E-[c(RGDfK)$_2$] demonstrated higher cytotoxicity effect than free DOX or the control conjugate. By showing the advantages of our conjugate which accumulates selectively at the tumor site, we hope to warrant it as a novel targeted, anti-angiogenic, and anticancer therapy.

Acknowledgements

The authors thank Merkel Technologies Ltd, David Merkel Golan and Ariel Roytman for their kind assistance using the ImageStream Multispectral Imaging flow Cytometer. DP is grateful to The Center for Nanoscience and Nanotechnology for their generous financial fellowship.

REFERENCES

[1] C. A. Garces, W. G. Cance, *Am. Surg.* **2004**, *70*, 565.
[2] V. Guarneri, P. F. Conte, *Eur. J. Nucl. Med. Mol. Imaging* **2004**, *31* (Suppl 1), S149.
[3] E. Miele, G. P. Spinelli, E. Miele, F. Tomao, S. Tomao, *Int. J. Nanomed.* **2009**, *4*, 99.
[4] L. A. Newman, S. E. Singletary, *Surg. Clin. North Am.* **2007**, *87*, 499.
[5] R. B. Weiss, *Semin. Oncol.* **1992**, *19*, 670.
[6] G. Minotti, P. Menna, E. Salvatorelli, G. Cairo, L. Gianni, *Pharmacol. Rev.* **2004**, *56*, 185.
[7] F. M. Muggia, M. D. Green, *Crit. Rev. Oncol. Hematol.* **1991**, *11*, 43.
[8] V. B. Pai, M. C. Nahata, *Drug Saf.* **2000**, *22*, 263.
[9] P. K. Singal, N. Iliskovic, T. Li, D. Kumar, *Faseb J.* **1997**, *11*, 931.
[10] D. Outomuro, D. R. Grana, F. Azzato, J. Milei, *Int. J. Cardiol.* **2007**, *117*, 6.
[11] K. Miller, R. Satchi-Fainaro, *Wiley Encyclopedia of Chemical Biology* (Ed.: N. R. Civjan), Vol. *3*, John Wiley & Sons, Inc, Weinheim, Germany. **2009**, 783.
[12] P. A. Vasey, S. B. Kaye, R. Morrison, C. Twelves, P. Wilson, R. Duncan, A. H. Thomson, L. S. Murray, T. E. Hilditch, T. Murray, *et al. Clin. Cancer Res.* **1999**, *5*, 83.
[13] R. C. Leonard, S. Williams, A. Tulpule, A. M. Levine, S. Oliveros, *Breast* **2009**, *18*, 218.
[14] E. Mrozek, C. A. Rhoades, J. Allen, E. M. Hade, C. L. Shapiro, *Ann. Oncol.* **2005**, *16*, 1087.
[15] A. Gabizon, D. Goren, Z. Fuks, A. Meshorer, Y. Barenholz, *Br. J. Cancer* **1985**, *51*, 681.
[16] R. Haag, F. Kratz, *Angew. Chem. Int. Ed. Engl.* **2006**, *45*, 1198.
[17] N. J. Robert, C. L. Vogel, I. C. Henderson, J. A. Sparano, M. R. Moore, P. Silverman, B. A. Overmoyer, C. L. Shapiro, J. W. Park, G. T. Colbern, *et al. Semin. Oncol.* **2004**, *31*, 106.
[18] H. Maeda, *Adv. Enzyme Regul.* **2001**, *41*, 189.
[19] Y. Matsumura, H. Maeda, *Cancer Res.* **1986**, *46*, 6387.
[20] D. Hanahan, J. Folkman, *Cell* **1996**, *86*, 353.
[21] E. Segal, R. Satchi-Fainaro, *Adv. Drug Deliv. Rev.* **2009**, *61*, 1159.
[22] J. Folkman, *N. Engl. J. Med.* **1971**, *285*, 1182.
[23] T. Browder, C. E. Butterfield, B. M. Kraling, B. Shi, B. Marshall, M. S. O'Reilly, J. Folkman, *Cancer Res.* **2000**, *60*, 1878.
[24] K. Miller, R. Erez, E. Segal, D. Shabat, R. Satchi-Fainaro, *Angew Chem. Int. Ed. Engl.* **2009**, *48*, 2949.
[25] J. Folkman, *Nat. Rev. Drug Discov.* **2007**, *6*, 273.
[26] J. Folkman, *Angiogenesis: An integrative approach from science to medicine* (eds: W. Figg, J. Folkman), Chapter 1, Springer-Verlag, Heidelberg, Germany, **2008**, 1.
[27] K. Temming, R. M. Schiffelers, G. Molema, R. J. Kok, *Drug Resist. Updat.* **2005**, *8*, 381.
[28] D. Hanahan, R. A. Weinberg, *Cell* **2000**, *100*, 57.
[29] P. C. Brooks, R. A. Clark, D. A. Cheresh, *Science* **1994**, *264*, 569.
[30] B. Felding-Habermann, B. M. Mueller, C. A. Romerdahl, D. A. Cheresh, *J. Clin. Invest.* **1992**, *89*, 2018.
[31] S. Zitzmann, V. Ehemann, M. Schwab, *Cancer Res.* **2002**, *62*, 5139.
[32] L. Bello, M. Francolini, P. Marthyn, J. Zhang, R. S. Carroll, D. C. Nikas, J. F. Strasser, R. Villani, D. A. Cheresh, P. M. Black, *Neurosurgery* **2001**, *49*, 380.
[33] C. Brakebusch, D. Bouvard, F. Stanchi, T. Sakai, R. Fassler, *J. Clin. Invest.* **2002**, *109*, 999.
[34] D. Meitar, S. E. Crawford, A. W. Rademaker, S. L. Cohn, *J. Clin. Oncol.* **1996**, *14*, 405.
[35] S. Sengupta, N. Chattopadhyay, A. Mitra, S. Ray, S. Dasgupta, A. Chatterjee, *J. Exp. Clin. Cancer Res.* **2001**, *20*, 585.
[36] K. Meerovitch, F. Bergeron, L. Leblond, B. Grouix, C. Poirier, M. Bubenik, L. Chan, H. Gourdeau, T. Bowlin, G. Attardo, *Vascul. Pharmacol.* **2003**, *40*, 77.
[37] C. C. Kumar, *Curr. Drug Targets* **2003**, *4*, 123.
[38] M. Janssen, W. J. Oyen, L. F. Massuger, C. Frielink, I. Dijkgraaf, D. S. Edwards, M. Radjopadhye, F. H. Corstens, O. C. Boerman, *Cancer Biother. Radiopharm.* **2002**, *17*, 641.
[39] M. L. Janssen, W. J. Oyen, I. Dijkgraaf, L. F. Massuger, C. Frielink, D. S. Edwards, M. Rajopadhye, H. Boonstra, F. H. Corstens, O. C. Boerman, *Cancer Res.* **2002**, *62*, 6146.
[40] M. J. Roberts, M. D. Bentley, J. M. Harris, *Adv. Drug Deliv. Rev.* **2002**, *54*, 459.
[41] A. Abuchowski, T. van Es, N. C. Palczuk, F. F. Davis, *J. Biol. Chem.* **1977**, *252*, 3578.
[42] M. Firon, M. Shaharabany, R. T. Altstock, J. Horev, A. Abramovici, J. H. Resau, G. F. Vande Woude, I. Tsarfaty, *Oncogene* **2000**, *19*, 2386.
[43] B. Larrivee, A. Karsan, *Methods Mol. Biol.* **2005**, *290*, 315.
[44] A. Gabizon, A. T. Horowitz, D. Goren, D. Tzemach, F. Mandelbaum-Shavit, M. M. Qazen, S. Zalipsky, *Bioconjug. Chem.* **1999**, *10*, 289.
[45] E. Segal, H. Pan, P. Ofek, T. Udagawa, P. Kopeckova, J. Kopecek, R. Satchi-Fainaro, *PLoS One* **2009**, *4*, e5233.
[46] C. Ryppa, H. Mann-Steinberg, M. L. Biniossek, R. Satchi-Fainaro, F. Kratz, *Int. J. Pharm.* **2009**, *368*, 89.
[47] V. J. Yao, M. G. Ozawa, A. S. Varner, I. M. Kasman, Y. H. Chanthery, R. Pasqualini, W. Arap, D. M. McDonald, *Cancer Res.* **2006**, *66*, 2639.
[48] A. Meyer, J. Auernheimer, A. Modlinger, H. Kessler, *Curr. Pharm. Des.* **2006**, *12*, 2723.
[49] C. Ryppa, H. Mann-Steinberg, I. Fichtner, H. Weber, R. Satchi-Fainaro, M. L. Biniossek, F. Kratz, *Bioconjug. Chem.* **2008**, *19*, 1414.
[50] M. P. Borgman, A. Ray, R. B. Kolhatkar, E. A. Sausville, A. M. Burger, H. Ghandehari, *Pharm. Res.* **2009**, *26*, 1407.
[51] M. P. Borgman, O. Aras, S. Geyser-Stoops, E. A. Sausville, H. Ghandehari, *Mol. Pharm.* **2009**, *6*, 1836.
[52] D. B. Pike, H. Ghandehari, *Adv. Drug. Deliv. Rev.* **2010**, *62*, 167.

